Origin of the visible absorption in radiation-resistant optical fibers

A. Morana,[1,2] M. Cannas,[2] S. Girard,[1] A. Boukenter,[1] L. Vaccaro,[2] J. Périsse,[3] J.-R. Macé,[4] Y. Ouerdane[1] and R. Boscaino[2]

[1] *Laboratoire H. Curien, UMR CNRS 5516, Université Jean Monnet, 18 rue du Pr. Benoît Lauras F-42000, Saint-Etienne, France*

[2] *Dipartimento di Fisica e Chimica, Università di Palermo, via Archirafi 36, I-90123 Palermo, Italy*

[3] *Areva NP, 10 rue Juliette Récamier F-69456 Lyon Cedex 06, France*

[4] *Areva, Tour Areva,1 place Jean Millier, F-92084 Paris La défense Cedex, France*

adriana.morana@univ-st-etienne.fr

Abstract: In this work we investigated the point defects at the origin of the degradation of radiation-tolerant optical fibers used in the visible part of the spectrum for plasma diagnostics in radiation environments. For this aim, the effects of γ-ray irradiation up to the dose of 10 MGy(SiO_2) and post-irradiation thermal annealing at 550°C were studied for a Fluorine-doped fiber. An absorption peaking around 2 eV is mainly responsible for the measured radiation-induced losses, its origin being currently debated in the literature. On the basis of the unchanging shape of this band with the radiation dose, its correlation with the 1.9 eV photoluminescent band and the thermal treatment results we assign the asymmetric absorption around 2 eV to an unique defect, the NBOHC, instead of a set of various defects.

OCIS codes: (060.2310) Fiber optics; (350.5610) Radiation; (250.5230) Photoluminescence; (300.1030) Absorption.

References and links

1. J. L. Bourgade, A. E. Costley, R. Reichle, E. R. Hodgson, W. Hsing, V. Glebov, M. Decreton, R. Leeper, J. L. Leray, M. Dentan, T. Hutter, A. Moroo, D. Eder, W. Shmayda, B. Brichard, J. Baggio, L. Bertalot, G. Vayakis, M. Moran, T. C. Sangster, L. Vermeeren, C. Stoeckl, S. Girard, and G. Pien, "Diagnostic components in harsh radiation environments: Possible overlap in R&D requirements of inertial confinement and magnetic fusion systems," Rev. Sci. Instrum. **79,** 10F304 (2008).
2. K. Kajihara, L. Skuja, M. Hirano, and H. Hosono, "Role of Mobile Interstitial Oxygen Atoms in Defect Processes in Oxides: Interconversion between Oxygen-Associated Defects in SiO_2 Glass," Phys. Rev. Lett. **92,** 1 (2004).
3. L. Skuja, "Optically active oxygen-deficiency-related centers in amorphous silicon dioxide," J. Non-Cryst. Solids **239,** 16–48 (1998).
4. K. Nagasawa, Y. Hoshi, Y. Ohki, and K. Yahagi, "Radiation effects on pure silica core optical fibers by γ-rays: relation between 2 eV band and Non-Bridging Oxygen Hole Centers," Jpn. J. Appl. Phys. **25,** 464–468 (1986).
5. K. Nagasawa, Y. Ohki, and Y. Hama, "Gamma-ray induced 2 eV optical absorption band in pure silica core fibers," Jpn. J. Appl. Phys. **26,** L1009–L1011 (1987).
6. D. L. Griscom and M. Mizuguchi, "Determination of the visible range optical absorption spectrum of peroxy radicals in gamma-irradiated fused silica," J. Non-Cryst. Solids **239,** 66–77 (1998).
7. D. L. Griscom, "γ-Ray-induced visible/infrared optical absorption bands in pure and F-doped silica-core fibers: are they due to self-trapped holes?," J. Non-Cryst. Solids **349,** 139–147 (2004).

8. Y. Sasajima and K. Tanimura, "Optical transitions of self-trapped holes in amorphous SiO_2," Phys. Rev. B **68,** 014204 (2003).
9. S. Girard, D.L. Griscom, J. Baggio, B. Brichard, and F. Berghmans, "Transient optical absorption in pulsed-X-ray-irradiated pure-silica-core optical fibers: Influence of self-trapped holes," J. Non-Cryst. Solids **352,** 2637–2642 (2006).
10. B. Brichard, A. Fernandez Fernandez, H. Ooms, P. Borgermans, and F. Berghmans, "Dependence of the POR and NBOHC defects as function of the dose in hydrogen-treated and untreated KU1 Glass Fibers," IEEE Trans. Nucl. Sci. **50,** 6, 2024–2029 (2003).
11. S. Girard, J.-P. Meunier, Y. Ouerdane, A. Boukenter, B. Vincent, and A. Boudrioua, "Spatial distribution of the red luminescence in pristine, gamma rays, and ultraviolet-irradiated multimode optical fibers," Appl. Phys. Lett. **84,** 4215–4217 (2004).
12. L. Vaccaro, M. Cannas, S. Girard, A. Alessi, A. Morana, A. Boukenter, Y. Ouerdane, and R. Boscaino, "Influence of fluorine on the fiber resistance studied through the nonbridging oxygen hole center related luminescence," Appl. Phys. **113,** 193107 (2013).
13. M. Cannas and F.M. Gelardi, "Vacuum ultraviolet excitation of the 1.9 eV emission band related to nonbridging oxygen hole centers in silica," Phys. Rev. B **69,** 153201 (2004).
14. G. H. Sigel and M. J. Marrone, "Photoluminescence In As-Drawn and Irradiated Silica Optical Fibers: An Assessment of the Role of Non-Bridging Oxygen Defect Centers," J. Non-Cryst. Solids **45,** 235–247 (1981).
15. M. Cannas, L. Vaccaro, and B. Boizot, "Spectroscopic parameters related to non-bridging oxygen hole centers in amorphous SiO_2," J. Non-Cryst. Solids **352,** 203–208 (2006).
16. L. Vaccaro, M. Cannas, and R. Boscaino, "Phonon coupling of non-bridging oxygen hole center with the silica environment: Temperature dependence of the 1.9 eV emission spectra," J. Lumin. **128,** 1132–1136 (2008).
17. M. Leone, M. Cannas, and F. M. Gelardi, "Local dynamic properties of vitreous silica probed by photoluminescence spectroscopy in the temperature range 300 ± 4.5 K," J. Non-Cryst. Solids **232–234,** 514–519 (1998).
18. L. Vaccaro and M. Cannas, "The structural disorder of a silica network probed by site selective luminescence of the nonbridging oxygen hole centre," J. Phys. Condens. Matter. **22,** 235801 (2010).
19. S. Agnello, G. Buscarino, F. M. Gelardi, and R. Boscaino, "Optical absorption band at 5.8 eV associated with the E'_γ centers in amorphous silicon dioxide: Optical absorption and EPR measurements," Phys. Rev. B **77,** 195206 (2008).
20. M. León, P. Martín, A. Ibarra, and E. R. Hodgson, "Gamma irradiation induced defects in different types of fused silica," J. Nucl. Mater. **386–388,** 1034–1037 (2009).
21. P. Martín, M. León, A. Ibarra, and E. R. Hodgson, "Thermal stability of gamma irradiation induced defects for different fused silica," J. Nucl. Mater. **417,** 818–821 (2011).

1. Introduction

Nowadays the nuclear industry gives an increasing interest in the fiber optic technology for both remote handling, diagnostic and sensing applications. The optical components employed in the nuclear power plants or facilities devoted to the fusion studies [1] are exposed to a high level of radiation (neutrons and γ-rays) and operate at high temperatures (up to 700°C). Such a harsh combined environment influences the performances of the optical fibers. On the one hand, the irradiation causes transmission losses due to the formation of optically active point defects, mainly in the ultraviolet (UV) and visible parts of the spectrum where a lot of diagnostics operate. On the other hand, the temperature effect leads to partial or total optical-fiber-transparence recovering via defects annealing [2]. These effects are particularly relevant to an optical absorption (OA) around 2 eV (620 nm) that grows with the deposited dose and constitutes the main contribution to induced losses from 1.5 eV (800 nm) to 3.1 eV (400 nm). Several studies based on optical and ESR experiments [3–5] have pointed out that the most important defect absorbing around 2 eV is the non-bridging oxygen hole center, NBOHC (≡Si-O•), but its band shape has never been analyzed in detail. Nagasawa et al. [4, 5] have asserted that the peak and the FWHM values can change with the OH-group content. Later, in similar samples the presence of other absorptions have been proposed in the same spectral region, these bands have been attributed to: the peroxy radical, POR (≡Si-O-O•), [6] and the selftrapped holes, STH (≡Si-Ȯ-Si≡) [7–9]. The attempt to single out the absorption related to specific defects has been mainly based on the deconvolution of the OA lineshape in gaussian bands [10]. This limited approach does not consider the possibility of an asymmetric absorption band and it leaves

often the problem incompletely solved, because some gaussian band reported in literature has not been assigned to well defined defect structures yet. The study of photoluminescence (PL) properties helps to clarify the origin of the OA around 2 eV, or at least of one of its components, in optical fibers. In this spectral region, in fact, an emission induced by both drawing and irradiation is observed in the optical fibers [11, 12]. This PL band is peaked at 1.9 eV (650 nm), its lifetime is about 10 μs, and it has different excitation channels: 2.0 eV (620 nm), 4.8 eV (260 nm), and 6.5 eV (190 nm). Several experiments have unambiguously ascribed this red luminescence to NBOHCs [3, 13], however most of the PL studies was realized in silica bulk samples; its spectroscopic characteristics were only poorly investigated in fibers [14]. In this work we study the effects induced by gamma irradiation and thermal annealing on the absorption and time resolved PL properties of a radiation-resistant fiber, thanks to the Fluorine-doping. On the strength of the assignment of 1.9 eV PL to NBOHC we revise the literature models dealing with the OA around 2 eV.

2. Experimental Details

We investigated a F-doped silica fiber with a diameter of 125 μm and a core of 50 μm. This sample was γ-ray irradiated at the Brigitte ^{60}Co facility (SCK·CEN, Belgium), at three different total doses, 3, 5.5 and 10 MGy, with a dose-rate ranging between 10 and 25 kGy/h, at temperature ranging between 30 and 50°C. Some months after the irradiation, absorption measurements at room temperature were performed by using the cut-back method, which consists in taking the ratio between the signal transmitted by a great and a short lengths of the sample, without changing injection conditions. All the transmission spectra in the visible range were recorded using a halogen light source and a spectrometer QE65000 from Ocean Optics. To investigate the annealing effects, about 2 m of the irradiated samples were heated in air up to 550°C, with a heating rate of 10°C/min, and kept for 15 min at that temperature. The recorded optical transmission signal L(λ), at room temperature, was used to monitor the thermal treatment influence on the radiation induced attenuation (RIA), by calculating the difference spectra between the T annealed sample response L(λ, T_{ann}) and the non-treated $L_0(\lambda)$ one. Confocal microscopy-luminescence (CML) spectra were performed by a LabRam Aramis (Jobin-Yvon) spectrometer equipped by a He-Cd ion laser emitting at 3.82 eV (325 nm), a charge coupled device (CCD) camera and microtranslation stages. We used a 40$\times$ objective and a diaphragm diameter of 75 μm, which gives a spatial resolution of about 5 μm. Time resolved PL spectra were excited in the UV-visible range by using an optical parametric oscillator pumped by the third harmonic (3.55 eV - 350 nm) of a Nd:YAG laser (pulse width of 5 ns, repetition rate of 10 Hz) and equipped with a II harmonic generation nonlinear crystal. The laser beam was focused into the core of a stripped piece of fiber. The beam energy density was monitored at the laser exit. The emitted light was spectrally resolved by a grating with 300 grooves mm^{-1} and 500 nm blaze, the spectral slit bandwidth was set to be 10 nm. Spectra were acquired by a gated intensified CCD camera driven by a delay generator, setting the acquisition time width Δt, that is the amplitude of the acquisition window during which the CCD is enabled to reveal the light, and the delay T_D of the acquisition window with respect to the arrival of the laser pulse. The photoluminescence excitation (PLE) spectra were measured manually point by point by tuning the laser and recording the PL intensity normalized to the laser pulse energy. All the PL spectra were plotted in energy scale and therefore corrected for the monochromator dispersion.

3. Experimental results

Figure 1(a) displays RIA spectra in 3, 5.5 and 10 MGy γ-ray irradiated fibers. All the curves present an absorption band around 620 nm, which increases with the dose up to 5.6 dB/m, and an UV-tail above 480 nm. Figure 1(b) shows the annealing difference spectrum, as de-

fined in the previous section, for the most irradiated sample. The absorption band at 620 nm is completely annealed after the thermal treatment at 550°C. We note that the UV tail is not completely annealed: the residual attenuation at the wavelength of 400 nm is still around 1 dB/m. To investigate the correlation of the absorption band at 620 nm with NBOHC we perform PL measurements around 1.9 eV (650 nm) for pristine and γ-irradiated fibers at different doses. This PL is observed by using the CML setup under excitation at 3.82 eV (325 nm) (inset of Fig. 2). The integrated-PL-intensity from all the fiber-transverse-surface results linearly correlated with the absorption at 620 nm (fig. 2). We note that also the pristine fiber shows a weak 1.9 eV emission, its intensity agrees with an absorption lower than our experimental uncertainty (0.10 dB/m).

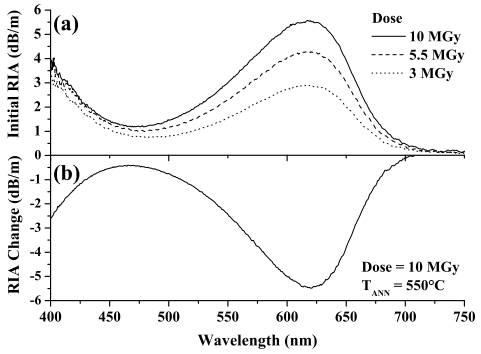

Fig. 1. (a) RIA spectra for the three doses γ-ray irradiated fibers. (b) RIA changes caused by thermal treatment at 550°C in the 10 MGy irradiated fiber irradiated.

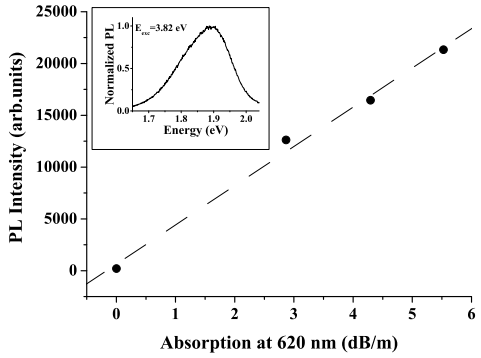

Fig. 2. PL intensity emitted from the fiber-transverse-surface of the samples, as a function of the optical absorption at 620 nm for pristine, 3, 5.5 and 10 MGy irradiated fibers. The dashed line is the fitted straight line (correlation coefficient R = 0.997). In the inset, the PL spectrum observed in the 10 MGy irradiated fiber, under excitation at 3.82 eV (325 nm).

In Fig. 3 we report the comparison between the time-resolved PL lineshape recorded in the pristine and in the 10 MGy irradiated fiber. The emission spectra were excited at E_{exc} = 2.07 eV (600 nm) and acquired with Δt = 10 μs and T_D = 1 μs. It is observed that after irradiation

the PL peak red-shifts from 1.92 to 1.90 eV and the FWHM increases from 0.15 to 0.17 eV.

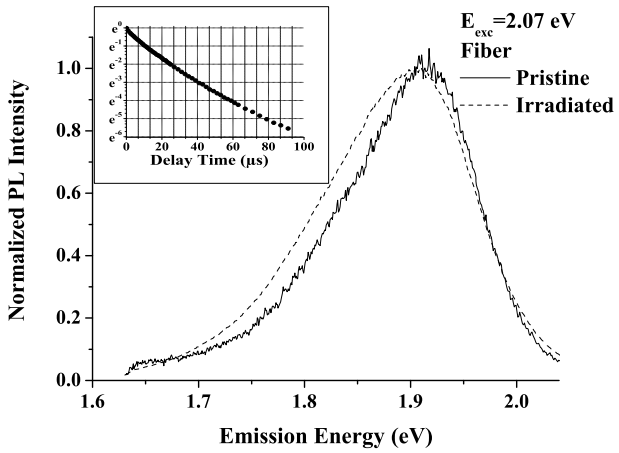

Fig. 3. Time-resolved PL spectra recorded on the pristine fiber (continuous line) and the irradiated one at the dose of 10 MGy (dotted line) under laser excitation at 2.07 eV (600 nm). The temporal parameters were fixed: T_D = 1 μs and Δt = 10 μs. Inset shows the semilog plot of the PL decay measured at 1.9 eV in the irradiated sample.

To measure the PL lifetime, we have carried out time resolved PL spectra on increasing T_D up to 90 μs with Δt ranging between 1 and 4 μs. In the insert of Fig. 3 the decay curve monitored at E_{em} = 1.9 eV in the irradiated sample is shown; it agrees with a stretched exponential $\exp(-(t/\tau)^{\beta})$ characterized by a lifetime τ = (11 $\pm$ 1) μs and a stretching parameter β = 0.81 $\pm$ 0.07. The stretching accounts for a rate distribution of defects embedded in a disordered structure. We observe that these decay features remain unchanged regardless the excitation energy both in the visible (2.0 eV) and in the UV (4.8 eV), after irradiation or thermal treatments (curves not shown here). Figure 4 shows the excitation profile of the PL at 1.9 eV, obtained by monitoring the peak emission intensity under laser excitation photon energy ranging from 1.7 to 2.3 eV. Both in the pristine and in the irradiated samples the visible excitation shows an asymmetric band centered at (1.95 $\pm$ 0.02) eV with FWHM of (0.16 $\pm$ 0.02) eV.

4. Discussion

RIA spectra in the visible range are dominated by a band around 2 eV (620 nm), that is completely bleached by the thermal treatment at 550°C. The origin of this absorption is still debated: one of the main questions concerns its assignment to a single or more defects. Under the hypothesis that more components overlap around 2 eV [6], we have analyzed all the spectra of Fig. 1 as a sum of three gaussian curves. The absorption above 2.8 eV (450 nm), due to the defects absorbing in the UV region, is accounted for by another gaussian centered around 5.5 eV. Figure 5 displays the decompositions of the RIA spectrum of the 10 MGy irradiated fiber; the spectral parameters are listed in table 1.

These results, derived from the fitting, agree with previous studies on thermally treated F-doped samples, both fibers and bulks. Griscom and Mizuguchi have attributed a band centered at 1.97 eV with FWHM of 0.18 eV to PORs, a band at 2.08 eV with FWHM of 0.3 eV to NBOHCs induced by the H removal from SiOH groups and a band at 2.19 eV band with FWHM of 0.5 eV to NBOHCs produced by the radiolysis of Si-O bonds [6]. However, some findings

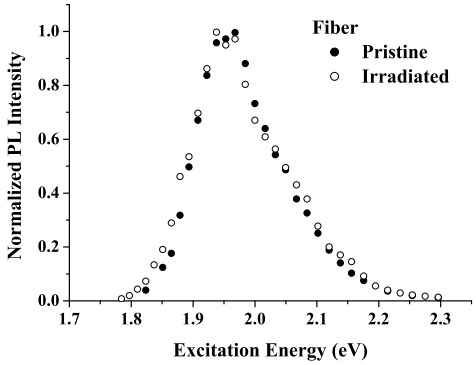

Fig. 4. Visible-excitation spectra of the PL at 1.9 eV measured with T_D = 1 μs and Δt = 10 μs in the pristine (full circles) and the 10 MGy irradiated sample (empty circles).

Table 1. Spectral parameters of the bands used for the decomposition of all the OA spectra recorded in 3, 5.5 and 10 MGy irradiated samples. The error accounts for half of the maximum deviation.

Band	Position (eV)	FWHM (eV)
1	1.945 ± 0.004	0.161 ± 0.011
2	2.04 ± 0.05	0.27 ± 0.08
3	2.21 ± 0.05	0.46 ± 0.06

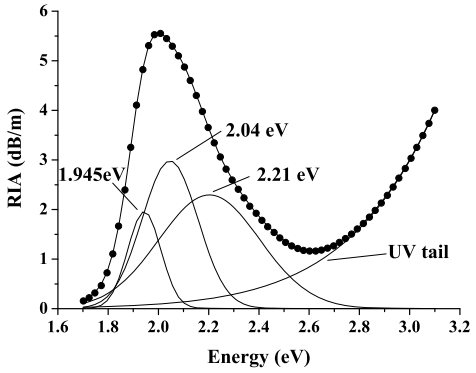

Fig. 5. Decomposition into gaussian bands of the RIA spectrum for the 10 MGy irradiated fiber: measured spectrum (dots) and fitted curve (lines).

weaken this model. Firstly, the absorption lineshape is independent of the radiation dose, so the production rate under radiation of the three defects should have to be exactly the same. Secondly, the 2 eV absorption is completely annealed at 550°C, consequently it seems unlikely a model containing an absorption band due to the PORs, whose annealing is completed around 700°C [2]. Finally, the OH concentration is not high enough to justify the 2.04 eV band intensity, associated with the NBOHCs deriving from the SiOH group, respect with that of the 2.21 eV component, due to the NBOHCs produced by the Si-O bonds rupture.

From the CML spectra we note that the 2 eV absorption band is linearly correlated to the emission at 1.9 eV. The identification of this emission with the NBOHC [3, 13] should carry that only this defect absorbs around 2 eV. This hypothesis has been already advanced in previous studies: for instance, Cannas et al. observed an asymmetric absorption band peaked at 2.01 eV with a FWHM of 0.44 eV in gamma and beta-irradiated synthetic wet silica samples and they associated it with NBOHCs thanks to its linear correlation with the PL at 1.9 eV [15]. The spectral and decay features evidenced by time resolved PL experiments support that the emitting defect in our F-doped fibers is the NBOHC. However, from a spectroscopic viewpoint, the acceptance of this single-defect model seems to be in contradiction with the different lineshapes between absorption and luminescence bands. It is known that the asymmetric PL and PLE spectra are accounted for by the weak electron-phonon coupling characteristics of the NBOHC. As a consequence, these bands can be described by a pekarian curve, which is the convolution of a gaussian and a poissonian and, under the straightforward model of coupling with a single mode of mean Huang-Rhys factor S and effective frequency ω, the lineshape $I(E)$ can be approximated by the function [16]:

$$I(E) \propto \sum_n \mathrm{e}^{-S} \frac{S^n}{n!} \exp\left[-\frac{(E - E_{00} \pm n\hbar\omega)^2}{2{\sigma_{inh}}^2} \right] \tag{1}$$

valid at temperature sufficiently low in order not to populate the higher vibrational levels, that is $KT \ll \hbar\omega$, where K is the Boltzmann constant. The signs $+$ and $-$ refer to the PL and PLE lineshape, respectively. Because of the glass disorder, the pure electronic transition between the lowest vibrational levels of the first excited and ground states is inhomogenously distributed in agreement with a gaussian curve, peaked at E_{00} with FWHM = $2\sqrt{2\ln(2)} \cdot \sigma_{inh}$. We used Eq. (1) to best fit the PL and PLE curves measured in irradiated samples, as shown in Fig. 6, and we get S = 1.3 $\pm$ 0.3, $\hbar\omega$ = (0.053 $\pm$ 0.009) eV, E_{00} = (1.93 $\pm$ 0.01) eV and FWHM = (0.082 $\pm$ 0.002) eV. We note that our spectra are detected at room temperature and $\hbar\omega \sim KT$, this introduces a further gaussian broadening adding to the inhomogenous one [17], that could be therefore overestimated by our fit procedure. In fact, σ_{inh} has been measured in previous works based on site selective luminescence [18] and it varies between 0.071 and 0.086 eV, depending on the irradiation history.

As concerns the absorption spectrum, its lineshape is much wider than the PLE one. Under the assumption that it is completely due to NBOHC, we can calculate the ratio between PLE and absorption, which is proportional to the quantum yield defined as the ratio between the number of emitted photons and of the absorbed ones. As shown in the inset of Fig. 6, it results in a photon energy dependent curve, thus suggesting that there are absorbing NBOHCs with non-radiative emission.

As final remarks, we observe that the irradiation induces a red-shift and a broadening in the PL spectra. Same behavior was observed by Vaccaro et al. for the PLE spectra associated with NBOHC in irradiated silica bulk samples [18]; in contrast, we note any change in the PLE spectra, probably because it is smaller than the error associated with the curve points. The shift of the absorption or PL bands to lower energies due to irradiation and the opposite shift due to thermal annealing have been also observed for other defects, like E′ ($\equiv$Si$^\bullet$) [19–

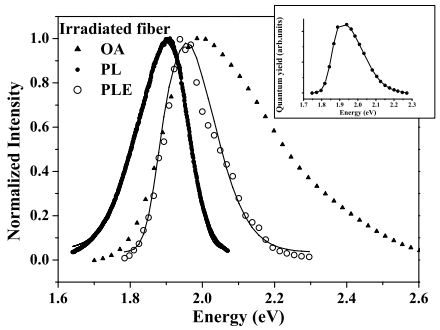

Fig. 6. Normalized PL, PLE and absorption spectra of the sample irradiated at 10 MGy. Solid curves represent the best-fitting functions (Eq. (1)). The inset shows the quantum yield calculated as the ratio between PLE and absorption.

21]: irradiation changes the environment of defects and high temperatures recover the pre-irradiated glass structure. The band broadening with irradiation can also be explained by an increasing disorder in the surroundings of NBOHCs [18]; the interaction between the defect and the environment does not affect the lifetime, which remains unchanged.

5. Conclusions

In this paper, we revise the origin of the 2 eV absorption band induced by radiation in the Fluorine-doped fibers, which limits the integration of these fibers as part of diagnostics or sensors in radiation environments. Thanks to the irradiation, the thermal treatment, RIA and PL measurements we discern between two models reported in literature: the first includes three centers (PORs and two different types of NBOHCs), whereas the second is based on only one defect, the NBOHC. From our results and analysis, we conclude that the RIA band around 2 eV has to be ascribed only to the NBOHC.